A Model for Simulation of the Energy Flows in a Heat Pipe Solar Collector

Boris Evstatiev[1], Nadezhda Evstatieva[2]
Department of Automatics and Electronics, University of Ruse "Angel Kanchev", Ruse, Bulgaria[1]
Laboratory Digital Energy Systems 4.0, University of Ruse "Angel Kanchev", Ruse, Bulgaria[2]

***Abstract*—The domestic sector is one of the major energy consumers and hot water is a compulsory service in modern society. Therefore, one of the possibilities for reducing energy expenses is heating water using solar collectors. However, the optimization of such installations requires careful planning and preliminary simulations. This study presents a model for simulating the energy flows in a heat pipe solar collector. Unlike previous studies, it also accounts for the self-shading of the vacuum tubes at certain hours of the day. An experimental setup was organized to collect reference data for model validation, and the data was automatically stored in a database by a microcontroller-based electronic system. The modeled and experimental data were compared and a PME of 1.55%, and a PMAE of 16.33% were obtained. The proposed model could be used for simulating the useful power of hybrid hot-water systems under different application scenarios.**

Keywords*—Model; simulation; heat pipe solar collector; useful power

I. INTRODUCTION

The domestic sector is one of the major energy consumers, responsible for 35% of the world's energy usage and 38% of the global direct and indirect CO_2 emissions [1]. Water heating is a requirement for modern society and therefore has a significant share in utility energy consumption. In this context, the integration of hybrid systems with renewable energy is an option to increase buildings' energy efficiency and to protect the environment [2].

Solar energy is widely used in hot water installations, because of its easy accessibility, high efficiency, and environment friendliness, which is especially important for modern society [3, 4]. The application of hybrid installations has proven its efficacy in improving energy sustainability [5]. Another reason for the increased interest towards them is the increased reliability and profitability, which overcomes the periodicity and uncertainties, related to solar energy [6]. Hybrid solar systems usually combine different renewable and non-renewable technologies, as well as storage of thermal energy [7]. The most common technologies used in hybrid systems for hot water are flat plate solar collectors and vacuum solar collectors [7-9], which are usually extended with conventional energy sources, such as electrical energy from the grid and LPG [10,11].

Numerous studies have investigated the application of flat-plate solar collectors (FPC) for heating water [12-15]. However, solar water heating systems (SWHS) rely on vacuum-based evacuated tube collectors (ETC), whose global share reaches up to 70% among all solar collectors [16]. ETCs can operate with high efficiency under cold and cloudy meteorological conditions and provide higher energy generation, making them better than FPCs [17]. For the abovementioned reasons, they are a common means of providing hot water in the utility sector [18,19]. In study [20] the efficiency of FPCs and ETCs were experimentally compared. According to the obtained results, vacuum solar collectors have significantly higher energy efficiency than flat-plate ones, which can be explained by the lower losses due to convective heat transfer.

To optimize the application of SWHS in practical situations, their energy output should be modeled and simulated, which is an object of investigation in many studies. In study [21] a model for two types of SWH systems is developed and validated. It relies on the transient systems simulation (TRNSYS) software. The main component of the model is a solar collector, based on either the flat plate technology or the vacuum-based heat pipe technology. For the FPC system, the study achieved average relative errors of the output collector temperature, the heat power, and the accumulated heat of 16.9%. 14.1%, and 6.9%, respectively. Similarly, for the ETC system, they are 18.4%, 16.8%, and 7.6%, respectively. The authors believe the model could be used for long-term forecasting of hot water systems and simulation of the system performance under different weather and operating conditions.

In another study, a heat transfer model of an all-glass vacuum tube collected was proposed in study [22]. The energy balance is formed by the natural convection in a single glass tube and forced convection in the collector, with the model estimating the temperature at the output of the collector. However, in this study, the shadows from one collector to the other are neglected, which might influence its accuracy. In study [23], a dynamic numerical model of a solar thermal installation with evacuated water heaters was presented. It was built in the TRNSYS18 environment and was aimed at forecasting solar energy gains. In another study [24] a theoretical model of an evacuated tube heat pipe solar collector with phase-change fluid was proposed. The solar water heating system contains a raw of ETC tubes, which are connected to a common manifold. The heat absorption and release modes are modeled using a combination of mathematical algorithms.

In study [25] an analytical thermal model of a solar water heater system was proposed, which is a combination of a heat pipe solar water heater system with phase-change material thermal energy storage. Approximate analytical solutions for

estimating the amount of absorbed solar energy and the thermal behavior of the supplied water were proposed. Similarly, in study [26] a model of vacuum solar collectors with a heat pipe was proposed, which is used in a solar desiccant cooling installation. After validation, the model was used to simulate the behavior of such an installation, used for cooling a building in the summer season under different climatic conditions.

Similarly, in study [27] TRNSYS was used to simulate the behavior of a forced circulation solar water heating system of a single-family house in Algeria. The study reported that the solar fraction of the system varied between 54% and 84% for the different months of the year. According to another study [28], industrial hybrid systems require uninterrupted access to hot water; i.e., an additional energy source, such as LPG and electrical energy should be provided. The authors presented a TRNSYS-based model of solar collectors in a hybrid system, allowing simulations for performance evaluation.

To ensure the efficient application of conventional energy and minimize the exploitation costs of a hybrid system for hot water production, it is necessary to choose an appropriate management strategy. This can be achieved by simulating different scenarios of the system's exploitation, which should be based on an appropriate model of the solar collectors.

The performed analysis showed that most of the previously developed models do not account for the shadows, dropped from one tube to the other, which might influence their accuracy in the evening and morning hours. Furthermore, it was observed that almost all authors from the last years have used the Transient System Simulation program (TRNSYS). While this tool supports shading simulation, it does not include an integrated solution that accounts for the self-shading from the heat-pipe solar collector.

This study aims to develop a model of the energy flows in a heat pipe solar collector, which allows us to estimate the thermal energy production for a certain level of solar radiation. The model should account for the self-shadings between the tubes of the collector and allow simulation of the instantaneous energy accumulated in the form of heat.

The rest of the paper is organized as follows: In Section II the methodology of the study is explained, and in Section III the experimental results are presented. In the final Section IV, conclusions are made about the accuracy and applicability of the study results.

II. Materials and Methods

A. Object of the Investigation

The objects of the investigation are the energy flows in glass vacuum tube collectors (see Fig. 1). In other words, the heat pipe is surrounded by a vacuum, ensured by a surrounding glass tube. Furthermore, the heat pipe is filled with heat transfer phase-change fluid, which condenses on the inner surface of the condenser and then returns to the sun-exposed base of the tube, and the main channel for energy transfer to the water heating chamber. This process continues as long as the vacuum solar collector is heated by the sun. Furthermore, in this study is assumed that the heat pipe is in contact with water, where the absorbed solar energy is "stored" in the form of heat.

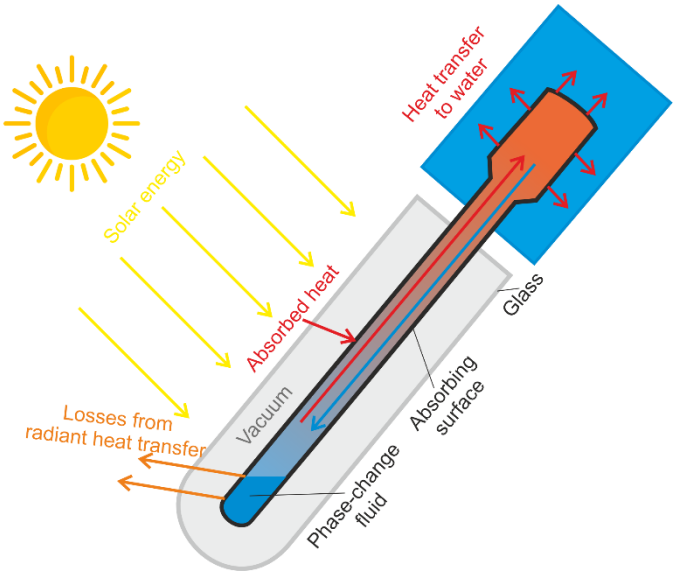

Fig. 1. Main energy flows in a vacuum solar collector with a heat pipe.

B. Energy Balance in a Vacuum Solar Collector with Heat Pipe

For the modeling purpose, it is accepted that the amount of energy gained by the solar collectors is proportional to the intensity of solar radiation and the surface of the solar collectors. Therefore, the receiving surface of a stationary solar collector is a function of its positioning in space and of the Sun's instantaneous location in the sky. The solar energy receiving surface depends on the total receiving surface of the collectors, the distance between their tubes, their azimuth and tilt angles, and the available solar irradiance. An additional factor that could influence their performance is dustiness; however, it is not an object for the current study.

To model the amount of energy, received from the Sun, it is accepted to be proportional to the amount of falling solar rays on the receiving surface, which is determined by projecting it on a surface, perpendicular to the solar rays. The movement of the Sun in the sky could be modelled using well-known dependencies and quantities, such as the study in [29]: the Sun declination; the geographic latitude; the hour angle ω; the solar azimuth angle A; the solar altitude angle h; the slope angle between the accepting surface plane and the horizontal plane S; the azimuth angle of the receiving surface γ; the direction of the solar radiation θ; and the angle between the normal plane of the receiving surface and the sun rays.

The power balance of the vacuum collector can be expressed with:

$$Q_{sol} - Q_{loss} = Q_{tube} + Q_{fl},\ W \quad (1)$$

where Q_{sol} is the available solar radiation in W, Q_{loss} are the losses due to radiant heat transfer from the heat pipe to the environment in W, Q_{tube} is the power used for heating the vacuum tube in W, and Q_{fl} is the power used for heating the water in W.

The solar power, accumulated in the vacuum solar collector can be estimated according to:

$$Q_{sol} = Q_S . F_{col} . k_{ref},\ W \quad (2)$$

where Q_S is the instantaneous value of the total solar irradiance, falling on the sloped receiving surface in $W.m^{-2}$, F_{col} is the projection of the vacuum solar collector' surface on the perpendicular plane to the solar rays in m^2, and k_{ref} is the reflection coefficient of the vacuum tube surface.

The maximum total solar irradiance for a certain geographic location, day of the year, and hour of the day are estimated according to well-known dependencies [30]. In the case of cloudiness, the reduced amount of solar energy could be estimated using an average cloudiness coefficient k_{cl} taking values between 0% and 100%:

$$Q_s = Q_{s.max} \frac{q_S^{100\%cl} + \left(q_S^{0\%cl} - q_S^{100\%cl}\right).\frac{100-k_{cl}}{100}}{q_S^{0\%cl}}, W \quad (3)$$

where $Q_{s.max}$ is the maximal possible solar radiation for the corresponding hour and day of the year W, $q_S^{100\%cl}$ and $q_S^{0\%}$ are the lowest (with maximal cloudiness) and highest (with lowest cloudiness) solar radiation rates in $W.m^{-2}$ for a certain month of the year at the corresponding time. The last two quantities can be obtained from archive meteorological data for the corresponding location.

C. Modelling of the Energy Flows in a Vacuum Solar Collector

To model the energy flows in a vacuum solar collector, the following basic approximations are accepted:

- The available solar irradiance reaching the vacuum solar tubes depends on the parameters of the Sun's movement on the horizon;
- The available energy is used for heating the elements of the construction, for heating the fluid, and for losses from radiant heat transfer;
- Considering the vacuum between the receiving surface and the glass tube, losses due to convective heat transfer are ignored;
- The energy entering the vacuum solar collector heats simultaneously the internal part of the tubes, the heat pipe, and the copper contact plate.

The solar energy, falling on a sloped surface is proportional to the projection of this surface over a plane, perpendicular to the solar rays. To determine the width of the projection b_{col}^{az}, the correction angles $-\alpha_{cor}$ and α_{cor}, and the solar azimuth angle should be accounted for. Fig. 2 summarizes the methodology for estimating the width of the projection, where 1, 2, and 3 are the active surfaces of the vacuum tubes.

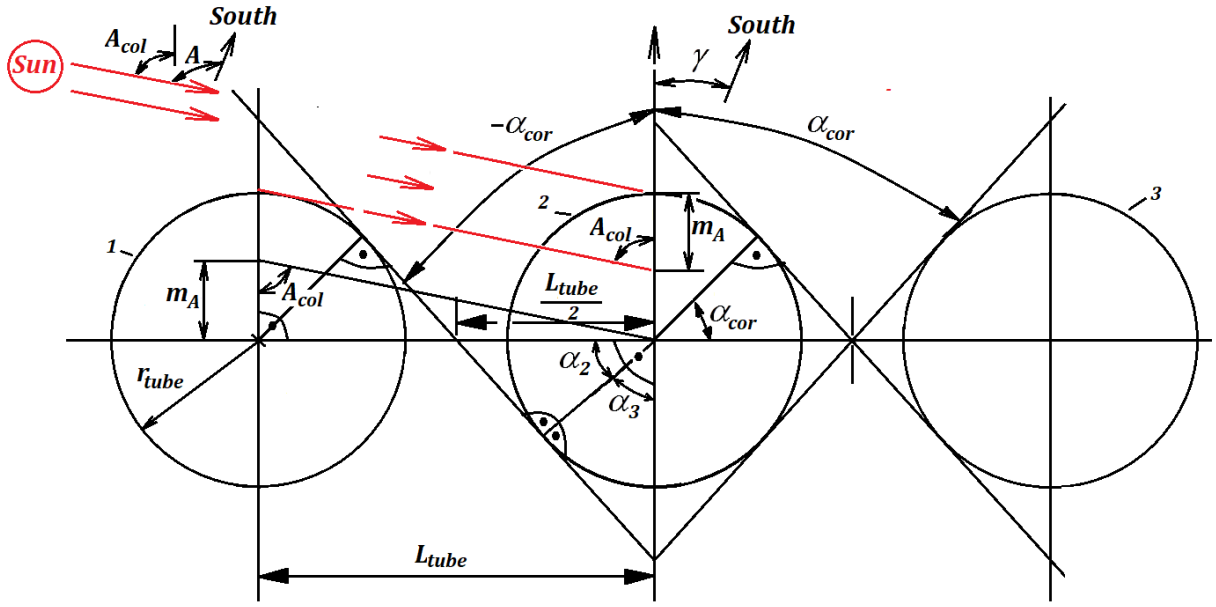

Fig. 2. Graphical representation of the methodology for estimating the width of the receiving surface projection.

It can be seen that whether the solar rays will fall on a certain tube depends on the angle A_{col}. The quantity $A_{col} = (A - \gamma)$ represents the difference between the azimuth angle of the Sun and the azimuth angle of the receiving surface, where the value of A_{col} is negative during sunrise and positive during sunset.

If A_{col} is within the zone $(-\alpha_{cor} \dots \alpha_{cor})$, the receiving surface of each tube is equal to its diameter d_{tube} in m and the total azimuth width of the solar collector is:

$$b_{col}^{az} = d_{tube} . n_{tube} \quad (4)$$

where n_{tube} is the number of tubes in the collector. At sunrise $A_{col} < -\alpha_{cor}$ and each tube partially shades the next one. In this case, the first tube is irradiated entirely, and the remaining ones only partially. When A_{col} is outside the zone $(-\alpha_{cor} \dots \alpha_{cor})$, the total width of the projection of the receiving surface on the perpendicular plane to the solar rays is:

$$b_{col}^{az} = d_{tube} + m_A . (n_{tube} - 1) \quad (5)$$

In this case $m_A = \frac{L_{tube}}{tg|A_{col}|}$ is the part of the diameter of the tube, corresponding to its irradiated surface and L_{tube} is the distance in m between the tubes. The dependency is the same during sunsets, when $A_{col} > \alpha_{cor}$.

To obtain the angle α_{cor} the following dependency can be used (see Fig. 2):

$$\alpha_{cor} = 90^o - \alpha_3 = 90^o - (90^o - \alpha_2) \quad (6)$$

The cosine of the angle α_2 is calculated according to:

$$cos\ \alpha_2 = \frac{r_{tube}}{L_{tube}/2} \quad (7)$$

where r_{tube} is the radius of the absorbing tubes inside the solar collector in m. By combining Eq. (6) and Eq. (7), the value of α_{cor} is estimated with:

$$\alpha_{cor} = 90^o - \left(90^o - \text{acos}\left(\frac{r_{tube}}{\frac{L_{tube}}{2}}\right)\right) = \text{acos}\left(\frac{r_{tube}}{\frac{L_{tube}}{2}}\right) \quad (8)$$

The algorithm for modeling the energy flows in a vacuum solar collector with a heat pipe during a certain day of the year is summarized in Fig. 3. It begins with block 1, where the initial conditions are set: the day of the year, the cloudiness coefficient, the latitude, the tilt and azimuth angles of the solar collectors, as well as other parameters of the solar collector. Next, in block 2 are estimated the general parameters of the Sun trajectory, which depend on the latitude and the day of the year, as well as of the solar collectors: the declination, the duration of sunlight, the hour angles, the sunrise and sunset hours, as well as the correcting angles -α_{cor} and α_{cor}, which depend on the distance between the tubes and their diameters.

In block 3 are set the initial values of some of the model parameters, which vary over the day, such as the initial time, the hour angle of the Sun, the initial temperature of the vacuum tubes, and of the fluid, and in block 4 are modified the cycle-controlled variables.

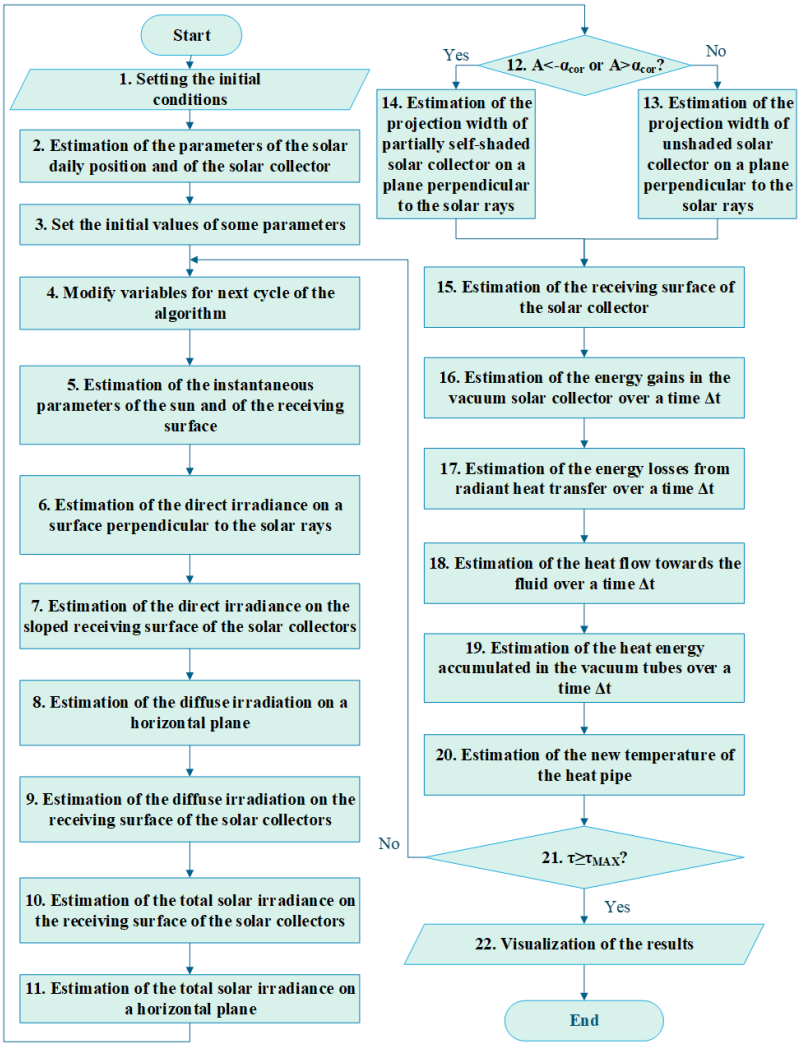

Fig. 3. Algorithm for modeling the energy flows in a vacuum solar collector with heat pipe.

Each cycle continues with block 5, where the instantaneous parameters of the Sun's position and the receiving surface are estimated for a certain time of the day: the elevation angle of the Sun, the azimuth of the Sun, and the direction of the direct irradiation relative to the receiving surface. Next, in blocks 6 and 7 the intensity of the direct irradiance, respectively on a

perpendicular plane and the receiving surface are estimated. Similarly, in blocks 8 and 9 the diffuse irradiance on a plane perpendicular to the solar rays and the receiving surface are obtained. In blocks 10 and 11 the total solar irradiance, falling respectively on the receiving surface of the solar collectors and a horizontal plane are evaluated.

In block 12 is verified whether the solar collector is partially self-shading itself. If no self-shading occurs, the algorithm continues to block 13, where the projected width of an unshaded receiving surface on a plane perpendicular to the solar rays is estimated by Eq. (4). Otherwise, Eq. (5) is applied in block 14 to evaluate the projected width of the self-shaded receiving surface.

In block 15, the surface of the solar collector using the following equation is estimated with:

$$F_{col} = b_{col}^{az}.c_{col},\ \ m^2 \tag{9}$$

where c_{col} is the length of the vacuum tubes in m. Next, in block 16 the solar energy received by the vacuum solar collectors over a time interval $\Delta\tau$ is estimated, according to Eq. (3). In block 17 the energy losses to the environment due to radiant heat transfer are estimated and in block 18 the energy accumulated into the fluid of the collector is obtained:

$$E_{fl} = Q_{fl}.\Delta\tau,\ \ J \tag{10}$$

where Q_{fl} is the power accumulated in the fluid in W. It can be estimated according to:

$$Q_{fl} = F_{hp}.\alpha_{hp}.(t_{hp} - t_{fl}),\ \ W \tag{11}$$

where F_{hp} is the contact surface of the heat pipe with the fluid in m^2 and α_{hp} is the convective heat transfer coefficient with the fluid in $W.m^{-2}.K^{-1}$. In this study, it is accepted that the temperature of the fluid is constant.

Next, in block 19 is estimated the energy, accumulated in the vacuum tubes E_{tube}, based on the energy balance, described with Eq. (6). The cycle is concluded in block 20, where the new temperature of the heat pipe is obtained using a calorimetric equation:

$$t_{hp}^{cur} = t_{hp}^{pr} + \frac{E_{tube}}{m_{glass}.c_{glass}+m_{copper}.c_{copper}+m_{hp}.c_{copper}},°C, \tag{12}$$

where t_{hp}^{pr} is the temperature of the tube in the previous moment in $°C$; m_{glass}, m_{copper}, and m_{hp} are the masses, respectively of the glass part, of the copper contact folio, and of the heat pipe of the vacuum tubes in kg; c_{glass} and c_{copper} are the specific heat capacities, respectively of glass and copper in $J.kg^{-1}.K^{-1}$.

If the maximal time of the simulation has not been reached, the algorithm returns to block 4. Otherwise, all obtained results are visualized to the user in block 22 and the algorithm is concluded.

D. Methodology for Verification of the Model

The model can be validated by comparing its results with experimentally obtained ones. Therefore, an experimental setup was created, whose structure and organization are summarized in Fig. 4. It includes the following components:

- Two vacuum tubes with heat pipes, which accept solar radiation;
- A third vacuum tube that is used only as a source of shading;
- An insulated heating chamber, which accepts the available energy from the vacuum tubes and accumulates it in the water in the form of heat;
- A water tank, which is used as a source of cold water for the system;
- A circulation pump, which is used to periodically replace the hot water in the heating chamber with cold one;
- Two temperature sensors, used for monitoring the temperature of the water in the heating chamber and of the environment, respectively;
- A microcontroller system, responsible for obtaining the sensors' readings and controlling the circulation pump. The temperature measurement is implemented over a 1-Wire interface using one digital I/O each and the turning on and off the pump is implemented over a digital output;
- A database on a nearby laptop for storing the process information. The communication between the microcontroller and the laptop is implemented over a serial interface.

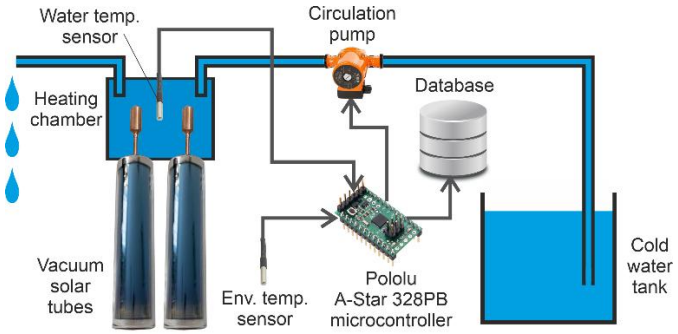

Fig. 4. Overview of the experimental system for verification of the vacuum solar collector model.

The system operates according to the following procedure. The microcontroller reads the temperature readings periodically. Thereafter, the changes in the temperature of the water and the losses to the environment are accounted for, so that the microcontroller can estimate the energy gain by the vacuum solar collectors between two consecutive readings. The power losses from the heating chamber to the environment are estimated by accounting for its insulation parameters and the temperature difference between the water and the environment, according to:

$$Q_{loss.exp} = \frac{T_{water}-T_{env}}{\frac{\delta_{wall}}{\lambda_{wall}}}.F_{wall},\ \ W, \tag{13}$$

where δ_{wall} is the width of the chamber's wall in m, λ_{wall} is the wall's thermal conductivity coefficient in $W.m^{-1}.K^{-1}$, and F_{wall} is the total wall surface of the chamber in m^2.

When the water temperature gets higher than a certain threshold, the circulation pump is started and the hot water is replaced with cold water, to prevent boiling. The average heat power Q_{tube} accumulated in the hot water over the period $\Delta\tau$ reduced with the heat losses Q_{loss}, is estimated with:

$$Q_{tube.exp} = \frac{m_{fl}.C_{fl}.\left(T_{fl}^{+\Delta\tau} - T_{fl}\right)}{\Delta\tau}, W, \quad (14)$$

where m_{fl} is the mass of the heating chamber water in kg, C_{fl} is the specific heat capacity of the fluid, which in this case is $C_{fl} = 4186\, J.kg^{-1}.K^{-1}$, T_{fl} is the fluid temperature at the beginning of the period and $T_{fl}^{+\Delta\tau}$ - $\Delta\tau$ seconds later, both in K.

All measured and estimated values are stored in the database, located on the laptop. The acquired heat flow $Q_{tube.exp}$, accumulated in the water is compared with the modeled one to assess the model's accuracy. This is done using two measures - percentage mean absolute error (PMAE) and percentage mean error (PME), estimated accordingly with:

$$PMAE = \frac{100}{N}\sum_{i=1}^{N}\frac{|A_{sim} - A_{mes}|}{A_{mes}}, \% \quad (15)$$

and

$$PME = \frac{100}{N}\sum_{i=1}^{N}\frac{A_{sim} - A_{mes}}{A_{mes}}, \%, \quad (16)$$

- where A_{sim} and A_{mes} are the simulated and measured values, respectively, and N is the total number of compared records.

III. Results and Discussion

A. Results from the Experimental Study

The verification of the developed model was performed by conducting an experimental study in the city of Ruse, Bulgaria, located at latitude $43{,}85^{o}N$ and longitude $25{,}97^{o}E$. The experimental setup was installed on the roof of Building 2 of the University of Ruse "Angel Kanchev" (Fig. 5), following the presented methodology for verification of the model. The experiment was conducted on 26.09.2023. In addition to the experimental setup, a Vantage Pro2 Plus meteorological station by Davis Instruments was used to monitor the environmental parameters. During the day the ambient temperature varied between 15 °C and 29.4 °C and the solar radiation reached up to 639 $W.m^{-2}$ around noon. No cloudiness was observed during this day; i.e., the used cloudiness coefficient is 0%.

Fig. 5. Geographic location of the experimental setup: a) Approximate location on the Bulgarian map; b) Exact location on the roof of Building 2 of the University of Ruse.

(a) (b)

Fig. 6. General view of the experimental setup for investigating the energy yield by a vacuum solar collector (a) and a closeup of the water chamber (b).

The experimental setup is characterized with the following key parameters (Fig. 6):

- The volume of the water in the heating chamber is 0.7 l.
- The insolation of the water chamber was implemented on two levels: 9 mm rubber was used to limit the convective heat transfer, and tinfoil was used to limit the influence of solar radiation on the temperature of the water.
- The used temperature sensors are DS18B20 by Dallas Semiconductors, which are characterized with 0.5 °C accuracy from -10°C to +85°C and 0.1 °C resolution.
- The used circulation pump has a debit of 0.4 $l.m^{-1}$.
- The two vacuum tubes are of type SPU-H58/1800-30-C by SunPower (China), characterized with 0.92 transmittance of the glass, 0.94 absorbance of the coating, and 0.08 hemispherical emittance.
- The azimuth and tilt angle of the vacuum tubes are 0° and 60°, respectively.

The characteristics of the parameters of the installation, used in the simulation are summarized in Table I. The electronic system has been operating as described in the methodology. The time series of the temperature readings during the sunny part of the day with approximately 19-20 s step of discretization is presented in Fig. 7. It can be seen that during the day the water in the heating chamber was replaced 39 times; i.e., the temperature of approximately 27.3 l was increased by approximately 22 °C.

Based on the proposed methodology and Eq. (12) and Eq. (13) the time series of the power accumulation in the heated water was obtained (Fig. 8). It can be seen that for the period from 9:00 to 18:30, the power absorbed in the water in the form of heat varies between 15 W in the morning/evening and 135 W around noon. The power accumulation process varied without sudden changes as the experiment was conducted on a sunny day with no cloudiness.

TABLE I. SUMMARY OF THE EXPERIMENTAL INSTALLATION PROPERTIES

№	Parameter	Value
1.	Specific heat capacity of water	4186 $J.kg^{-1}.K^{-1}$
2.	Specific heat capacity of the water chamber (made of PVC)	900 $J.kg^{-1}.K^{-1}$
3.	Convective heat transfer coefficient between the water chamber's inner walls and the water	400 $W.m^2.K$
4.	Convective heat transfer coefficient between the water chamber's outer walls and the environment	5.6 $W.m^2.K$
5.	Thermal conductivity coefficient of the water heat wall (PVC)	0.15 $W.m^{-1}.K^{-1}$
6.	Thermal conductivity coefficient of the water chamber insulation (rubber)	0.16 $W.m^{-1}.K^{-1}$
7.	Width of the water chamber insulation	0.0090 m
8.	The total surface of the water chamber	0.060 m^2
9.	Mass of the fluid	0.69 kg
10.	Mass of the water chamber	0.082 kg
11.	The radius of the vacuum tubes	0.029 m
12.	Length of the vacuum tubes	1.75 m
13.	Distance between the axes of the vacuum tubes	0.07 m
14.	Number of vacuum tubes	2
15.	Mass of a vacuum tube without the heat pipe (the glass)	2 kg
16.	Mass of the heat pipe of a vacuum tube	0.33 kg
17.	Specific heat capacity of glass	84 $J.kg^{-1}.K^{-1}$
18.	Specific heat capacity of copper	385 $J.kg^{-1}.K^{-1}$
19.	Total exchange surface of the two heat pipes with the water	0.0061 m^2

B. Validation of the Developed Model

The proposed model for simulation of the energy flows in a heat pipe solar collector was implemented in a software tool, developed in the Microsoft Visual Studio 2019 environment. To validate the developed model, the modeled heat accumulated by the solar collectors should be compared with the experimentally obtained. The model's parameters used during the simulation are selected following the used hardware components, as shown in Table I.

As was already mentioned, for the investigated day no cloudiness was observed. This is also confirmed by the maximal measured solar radiation (639 $W.m^{-2}$), which is almost identical to the theoretically maximal value for this geographic location and day of the year (659 $W.m^{-2}$). According to the developed methodology, the power accumulated by the fluid is estimated with a 5-minute time step, which is thereafter compared with the experimentally obtained one.

The integrated fluid energy gain was obtained similarly - according to the developed model and experimentally. The time series of the powers and daily energy gains are summarized in Fig. 9. It can be seen that the experimentally obtained and modeled quantities generally correspond very well. Furthermore, the daily cumulative heat gain is almost identical: 0.97 kWh and 0.96 kWh, obtained experimentally and via simulation, respectively. This corresponds to a 1% relative error at the end of the day.

Nevertheless, to get a better understanding of the difference, the absolute errors in the power and energy gains were evaluated and summarized in Fig. 10. It can be seen that the errors in the instantaneous power vary from -40 W to +20 W, with peak values occurring mostly in the morning and evening hours. This could be explained by shadows, falling from nearby buildings, which were not accounted for by the model.

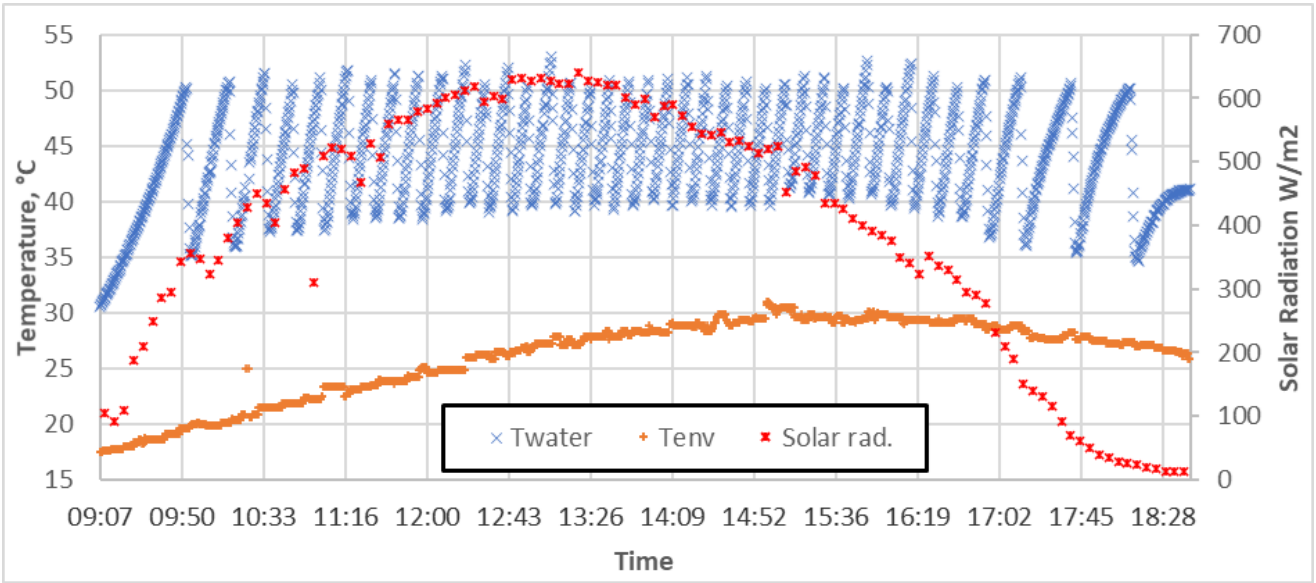

Fig. 7. Time series of the ambient temperature (orange), water temperature (blue) and solar radiation obtained from the meteorological station (red).

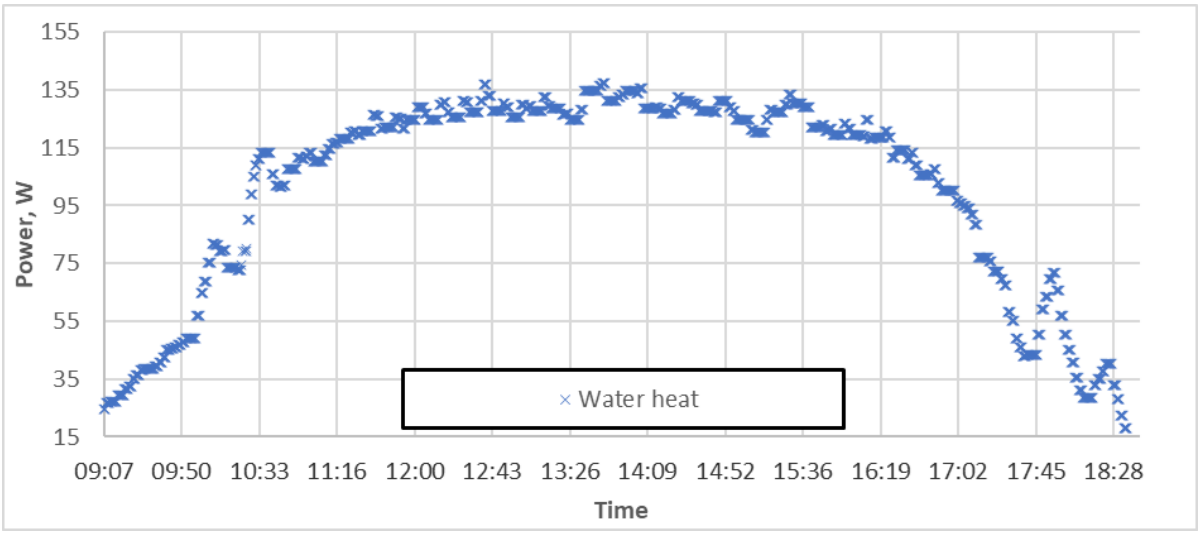

Fig. 8. Time series of the useful power, accumulated in the water.

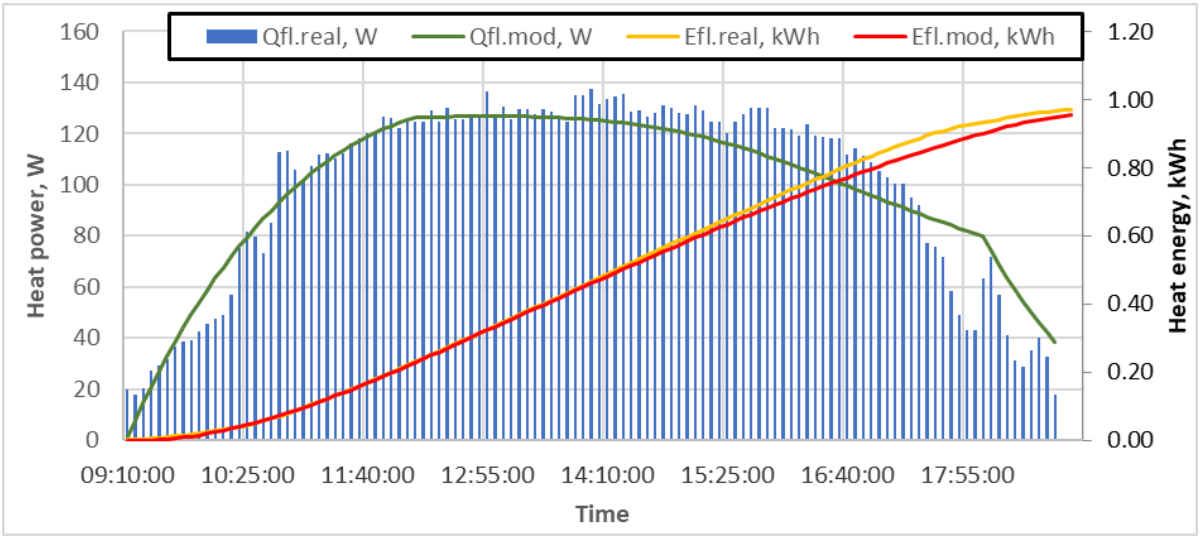

Fig. 9. Time series of: experimentally obtained heat power (blue), modeled heat power (green), experimentally obtained integrated heat energy (yellow), and modeled integrated heat energy (red).

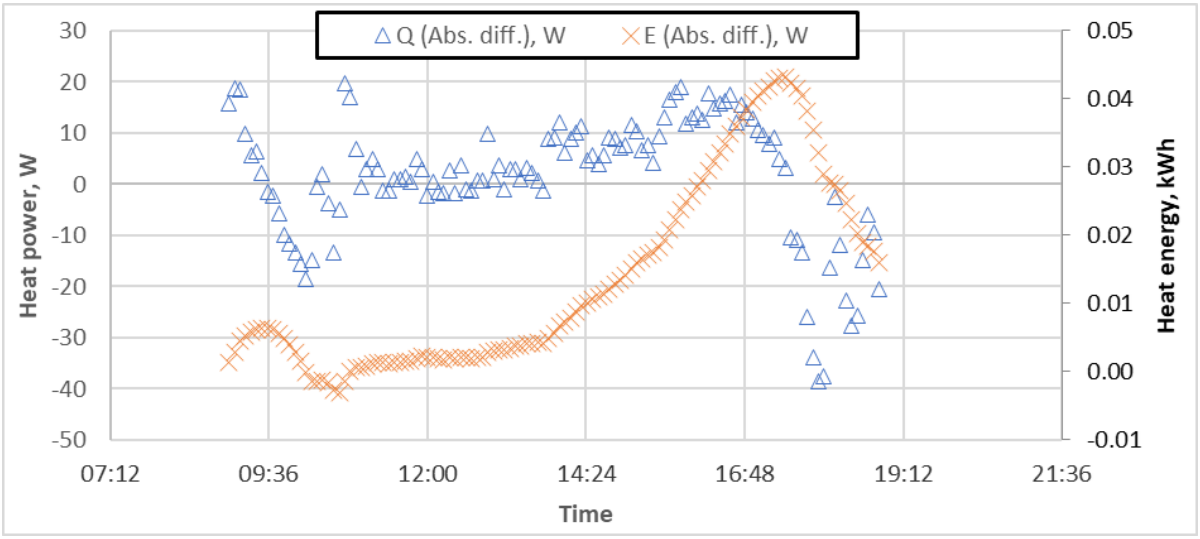

Fig. 10. Time series of the absolute errors of the heat power and heat energy gains during the experimental period.

The integrated daily energy gains are close to zero during the first half of the day and increase up to 0.04 kWh in the afternoon, though they fall back to 0.01 kWh at the end of the day. The obtained PME and PMAE measures for the heat power, absorbed by the water, are 1.55% and 16.33%, respectively. These values indicate that there are some errors in the obtained results with different signs, which compensate for each other, and at the end of the day the error is very low. Similarly, the PME and PMAE for the integrated accumulated energy are -7.69% and 8.02%, respectively. In this case, the difference between PME and PMAE is almost insignificant, because the errors in the integrated energy production are mostly with the same sign.

The model could be further evaluated by comparing its performance metrics with those obtained in previous studies. The authors of study [21] used a TRNSYS model to simulate the absorbed heat power in FPC and ETC systems. The achieved PME measures were 7.9% and 7.6%, respectively and the PMAE measures – 6.9% and 18.4%, respectively. In study [23] a numerical model in the TRNSYS environment was developed for simulating the temperature and energy gain from evacuated tube solar collectors. The study reported a PMAE of 8.02% for the daily energy production and a relative error of -0.2%. In another study [28], the output temperature of an FPC was simulated. The study reported a 2.01% root mean square error (RMSE) for the water's temperature; however, no error was reported for the estimated useful power. In general, it can be seen that the proposed model achieved similar results, as the previously developed in terms of PMAE, and higher accuracy when it comes to instantaneous power, measured with the PME metric. This indicates that the model could be used for simulating different scenarios of application of vacuum solar collectors, i.e. estimating their optimal regimes of exploitation.

A limitation of the proposed model is that it uses a cloudiness coefficient, to account for the available solar energy. This means that the obtained results might be inaccurate under dynamic meteorological conditions. Nevertheless, this should not affect the obtained results for long-term analysis as the errors would be with different signs and are expected to compensate for each other.

IV. Conclusions

In this study, a physical model for simulating the heat flows in a vacuum solar collector with a heat pipe was proposed. It is based on the power balance of the collector and accounts for its equivalent surface, the self-shading, and the position of the Sun. The model validation is performed by organizing an experimental study. A vacuum solar collector with two tubes was used to heat 0.7 *l* of water, which was periodically replaced with cold water. Based on the temperature changes, the useful power of the solar collectors was obtained and used as reference data for validating the model.

The obtained simulated values showed high correspondence with the experimentally obtained ones. The absolute power error is mostly around 0 W during the day and increases up to 40 W during the morning and evening hours. They can be explained by the shadows falling from nearby buildings, which were not accounted for in the model. The absolute errors of the cumulative useful energy vary between 0 and 0.04 kWh. The error at the end of the day is approximately 0.015 kWh, which corresponds to 1.6%.

These results indicate that the model can be used for precise simulation of the power and energy flows in a vacuum tube collector. It can be applied for forecasting the useful energy gains of vacuum collectors, as well as for optimization of water management in hybrid installations. Furthermore, it could be used to compare different scenarios in specific applications and to obtain the best-performing ones. The abovementioned is an object for our future studies.

Acknowledgment

This study is financed by the European Union-NextGenerationEU, through the National Recovery and Resilience Plan of the Republic of Bulgaria, project № BG-RRP-2.013-0001.

References

[1] M. Krarouch, A. Allouhi, H. Hamdi, A. Outzourhit, "Energy, exergy, environment and techno-economic analysis of hybrid solar-biomass systems for space heating and hot water supply: Case study of a Hammam building," Renewable Energy, vol. 222, 1-18, 119941, 2024. https://doi.org/10.1016/j.renene.2024.119941

[2] M. Karadjov and T. Hristova, "Application of SWOT Analysis for the Selection of a Hybrid System for Heating and Production of Energy and Hot Water for the Conditions of Bulgaria," 2023 18th Conference on Electrical Machines, Drives and Power Systems (ELMA), Varna, Bulgaria, 2023, pp. 1-4. https://doi.org/10.1109/ELMA58392.2023.10202503

[3] A. Elbrashy, Y. Boutera, M. M. Abdel-Aziz, S. Dafea, M. Arici, "A review on air heating applications with evacuated tubes: A focus on series and parallel tube configurations," Solar Energy, vol. 264, 1-26, 2023, 111996, https://doi.org/10.1016/j.solener.2023.111996

[4] S. K. Pathak, V. V. Tyagi, K. Chopra, and A. Sari, "Thermal performance and design analysis of U-tube based vacuum tube solar collectors with and without phase change material for constant hot water generation," Journal of Energy Storage, vol. 66, no. 107352, 2023. https://doi.org/10.1016/j.est.2023.107352

[5] K. Daghsen, A. Picallo Perez, D. Lounissi, N. Bouaziz, "Exergy, exergoeconomic and exergoenvironmental assessments of experimental hybrid energy systems for hot water production to improve energy sustainability," Renewable and Sustainable Energy Reviews, vol. 187, 1-18, 113741, 2023, https://doi.org/10.1016/j.rser.2023.113741

[6] Q. Hassan, Y. Algburi, A. Z. Sameen, H. M. Salman, M. Jaszczur, "A review of hybrid renewable energy systems: Solar and wind-powered solutions: Challenges, opportunities, and policy implications," Results in Engineering, vol. 20, 1-25, 101621, 2023, https://doi.org/10.1016/j.rineng.2023.101621

[7] E. Pérez-Iribarren, I. González-Pino, Z. Azkorra-Larrinaga, M. Odriozola-Maritorena, I. Gómez-Arriarán, "A mixed integer linear programming-based simple method for optimizing the design and operation of space heating and domestic hot water hybrid systems in residential buildings," Energy Conversion and Management, vol. 292, 1-24, 117326, 2023, https://doi.org/10.1016/j.enconman.2023.117326

[8] E. Dudkiewicz, N. Fidorów-Kaprawy, "The energy analysis of a hybrid hot tap water preparation system based on renewable and waste sources," Energy, vol. 127, pp. 198-208, 2017, https://doi.org/10.1016/j.energy.2017.03.061

[9] M. K. Abadi, V. Davoodi, M. Deymi-Dashtebayaz, A. Ebrahimi-Moghadam, "Determining the best scenario for providing electrical, cooling, and hot water consuming of a building with utilizing a novel wind/solar-based hybrid system," Energy, vol. 273, 127239, 2023, https://doi.org/10.1016/j.energy.2023.127239

[10] M. Baneshi, S. A. Bahreini, "Impacts of hot water consumption pattern on optimum sizing and techno-economic aspects of residential hybrid solar water heating systems," Sustainable Energy Technologies and

Assessments, vol. 30, pp. 139-149, 2018, https://doi.org/10.1016/j.seta.2018.09.008

[11] Z. Chen, C. Qin, Q. Jin, "Experimental and theoretical study on a hybrid residential hot water system with solar and gas," Journal of Natural Gas Science and Engineering, vol. 26, pp. 974-980, 2015, https://doi.org/10.1016/j.jngse.2015.07.037

[12] M. Carmona, M. Palacio, "Thermal modelling of a flat plate solar collector with latent heat storage validated with experimental data in outdoor conditions," Solar Energy, vol. 177, pp. 620-633, 2019, https://doi.org/10.1016/j.solener.2018.11.056

[13] Z. Badiei, M. Eslami, K. Jafarpur, "Performance improvements in solar flat plate collectors by integrating with phase change materials and fins: A CFD modeling," Energy, volume 192, 116719, 2020, https://doi.org/10.1016/j.energy.2019.116719

[14] Z. Hajabdollahi, H. Hajabdollahi, "Thermo-economic modeling and multi-objective optimization of solar water heater using flat plate collectors," Solar Energy, vol. 155, pp. 191-202, 2017, https://doi.org/10.1016/j.solener.2017.06.023

[15] A. Raul, M. Jain, S. Gaikwad, S.K. Saha, "Modelling and experimental study of latent heat thermal energy storage with encapsulated PCMs for solar thermal applications," Applied Thermal Engineering, vol. 143, pp. 415-428, 2018, https://doi.org/10.1016/j.solener.2017.06.023

[16] W.A. Fadzlin, M. Hasanuzzaman, N.A. Rahim, N. Amin, Z. Said, "Global Challenges of Current Building-Integrated Solar Water Heating Technologies and Its Prospects: A Comprehensive Review," Energies, vol. 15, no. 14. p. 5125, 2022, https://doi.org/10.3390/en15145125

[17] S. M. Tabarhoseini, M. Sheikholeslami, and Z. Said, "Recent advances on the evacuated tube solar collector scrutinizing latest innovations in thermal performance improvement involving economic and environmental analysis," Solar Energy Materials and Solar Cells, vol. 241, no. 111733, 2022. https://doi.org/10.1016/j.solmat.2022.111733

[18] X. Chen, X. Yang, "Heat transfer enhancement for U-pipe evacuated tube solar absorber by high-emissivity coating on metal fin," Journal of Building Engineering, vol. 50, 104213, 2022, https://doi.org/10.1016/j.jobe.2022.104213

[19] A. A. Khadom, H. B. Mahood, A. A. Mahmmod, Q. Hassan, H. A. Kazem, "Improving solar water heating performance and reducing emissions by evacuated tube collectors with preheating units: Iraq as a case study," Applied Thermal Engineering, vol. 265, 125596, 2025, https://doi.org/10.1016/j.applthermaleng.2025.125596

[20] M. Arsalan, M. Abid, M. Ali, J. Akhter, R. Kousar, J. H. Zaini, "Experimental development, techno-economic and environmental analysis of a hybrid solar space heating system in a subtropical climate," Energy Reports, vol. 10, pp. 3020-3034, 2023 https://doi.org/10.1016/j.egyr.2023.09.136

[21] L.M. Ayompe, A. Duffy, S.J. McCormack, M. Conlon, "Validated TRNSYS model for forced circulation solar water heating systems with flat plate and heat pipe evacuated tube collectors," Applied Thermal Engineering, vol. 31, no. 8–9, pp. 1536-1542, 2011, https://doi.org/10.1016/j.applthermaleng.2011.01.046

[22] Z. Li, C. Chen, H. Luo, Y. Zhang, Y. Xue, "All-glass vacuum tube collector heat transfer model used in forced-circulation solar water heating system," Solar Energy, vol. 84, pp. 1413–1421, 2010. https://doi.org/10.1016/j.solener.2010.05.001

[23] J. Gambade, H. Noël, P. Glouannec, A. Magueresse, "Numerical model of intermittent solar hot water production," Renewable Energy, vol. 218, 119368, 2023. https://doi.org/10.1016/j.renene.2023.119368

[24] M.S. Naghavi, K.S. Ong, I.A. Badruddin, M. Mehrali, M. Silakhori, H.S.C Metselaar, "Theoretical model of an evacuated tube heat pipe solar collector integrated with phase change material," Energy, vol. 91, pp. 911-924, 2015, https://doi.org/10.1016/j.energy.2015.08.100

[25] M.S. Naghavi, M. Silaakhori, M. Mehrali, H.S.C. Metselaar, I.A Badruddin, "Analytical thermal modeling of a heat pipe solar water heater system integrated with phase change material," Computer Applications in Environmental Sciences and Renewable Energy, pp. 197–208, 2014.

[26] P. Bourdoukan, E. Wurtz, P. Joubert, M. Spérandio, "Potential of solar heat pipe vacuum collectors in the desiccant cooling process: Modelling and experimental results," Solar Energy, vol. 82, no. 12, pp. 1209-1219, 2008, https://doi.org/10.1016/j.solener.2008.06.003

[27] A. Remlaoui, D. Nehari, B. Kada, et al., "Numerical simulation of a forced circulation solar water heating system," Sci Rep, vol. 14, no. 28999, 2024. https://doi.org/10.1038/s41598-024-80576-y

[28] L. Kumar, M. Hasanuzzaman, N.A. Rahim, M.M. Islam, "Modeling, simulation and outdoor experimental performance analysis of a solar-assisted process heating system for industrial process heat," Renewable Energy, vol. 164, pp. 656-673, 2021, https://doi.org/10.1016/j.renene.2020.09.062

[29] N. Ahmad, "MATLAB/Simulink Based Instantaneous Solar Radiation Modeling, Validation and Performance Analysis of Fixed and Tracking Surfaces for the Climatic Conditions of Lahore City, Pakistan," Int. J. Renew. Energy Dev., vol. 11, no. 3, pp. 608-619, 2022. https://doi.org/10.14710/ijred.2022.38748

[30] L. Wald, "Basics in solar radiation at earth surface," Lecture Notes, Ed. 1, 2018. hal-01676634, MINES ParisTech, PSL Research University, Sophia Antipolis, France. https://minesparis-psl.hal.science/hal-01676634/file/2018_basics_solaire_wald_v1.pdf